HHS Public Access

Author manuscript

Magn Reson Med. Author manuscript; available in PMC 2017 August 01.

Published in final edited form as:

Magn Reson Med. 2017 June ; 77(6): 2303–2309. doi:10.1002/mrm.26327.

Externally Calibrated Parallel Imaging for 3D Multispectral Imaging Near Metallic Implants Using Broadband Ultrashort Echo Time Imaging

Curtis N. Wiens[1,*], **Nathan S. Artz**[1,2], **Hyungseok Jang**[1,3], **Alan B. McMillan**[1], and **Scott B. Reeder**[1,4,5,6,7]

[1]Department of Radiology, University of Wisconsin, Madison, WI, USA

[2]Department of Diagnostic Imaging, St. Jude Children's St. Jude Children's Research Hospital, Memphis, TN, USA

[3]Department of Electrical and Computer Engineering, University of Wisconsin, Madison, WI, USA

[4]Department of Medical Physics, University of Wisconsin, Madison, WI, USA

[5]Department of Biomedical Engineering, University of Wisconsin, Madison, WI, USA

[6]Department of Medicine, University of Wisconsin, Madison, WI, USA

[7]Dept. of Emergency Medicine, University of Wisconsin, Madison, WI, USA

Abstract

Purpose—To develop an externally calibrated parallel imaging technique for three-dimensional multispectral imaging (3D-MSI) in the presence of metallic implants.

Theory and Methods—A fast, ultrashort echo time (UTE) calibration acquisition is proposed to enable externally calibrated parallel imaging techniques near metallic implants. The proposed calibration acquisition uses a broadband radiofrequency (RF) pulse to excite the off-resonance induced by the metallic implant, fully phase-encoded imaging to prevent in-plane distortions, and UTE to capture rapidly decaying signal. The performance of the externally calibrated parallel imaging reconstructions was assessed using phantoms and in vivo examples.

Results—Phantom and in vivo comparisons to self-calibrated parallel imaging acquisitions show that significant reductions in acquisition times can be achieved using externally calibrated parallel imaging with comparable image quality. Acquisition time reductions are particularly large for fully phase-encoded methods such as spectrally resolved fully phase-encoded three-dimensional (3D) fast spin-echo (SR-FPE), in which scan time reductions of up to 8 min were obtained.

Conclusion—A fully phase-encoded acquisition with broadband excitation and UTE enabled externally calibrated parallel imaging for 3D-MSI, eliminating the need for repeated calibration regions at each frequency offset. Significant reductions in acquisition time can be achieved, particularly for fully phase-encoded methods like SR-FPE.

[*]Corresponding author: Curtis Wiens, PhD, University of Wisconsin, Dept. of Radiology, 1111 Highland Ave, Room 1005, Madison WI 53705. cwiens@wisc.edu.

Keywords

metallic implant; parallel imaging; off-resonance; multispectral imaging; fully phase-encoded imaging

INTRODUCTION

Joint replacement surgery (arthroplasty) is a common procedure to treat degenerative joint disease. The number of joint replacement surgeries (eg, total hip replacements, total knee replacements) is increasing as a result of an aging population and an increasing incidence of osteoarthritis (1). Although arthroplasty is generally highly successful with good outcomes, prosthetic-related complications are common and include particle disease, pseudo-tumors, loosening (osetolysis), infection, synovitis, osteolysis, osteonecrosis, tendinopathy, fracture, and neurovascular impingement (2–4).

Detection of prosthetic-related complications using conventional MRI techniques is very limited. The large magnetic susceptibility difference between metallic implants and tissue generate severe B_0 inhomogeneities (5). These B_0 inhomogeneities present several challenges including RF excitation of the entire off-resonance spectrum, distortions in the frequency-encoding direction, and rapid intravoxel dephasing (6,7).

3D multispectral imaging (3D-MSI) techniques such as multi-acquisition with variable resonance image combination (MAVRIC) (8) and slice encoding for metal artifact correction (SEMAC) (9) can substantially reduce susceptibility-related artifacts. These techniques are both based on a Carr-Purcell-Meiboom-Gill (CPMG) spin-echo sequence. In SEMAC, the off-resonance induced by the combination of a slice-selective gradient and the metallic implant produces distorted slices that are resolved using through-plane phase encoding. In MAVRIC, multiple spin-echo acquisitions are acquired at different transmit and receive frequencies spanning the off-resonance spectrum induced by the implant. These techniques use high read-out bandwidths, low RF excitation bandwidths, and in the case of SEMAC and slab-selective MAVRIC (MAVRIC-SL (10)), view angle tilting to minimize distortions in the frequency-encoded direction that manifests as geometric distortions, signal pile-up, and signal void artifacts.

To avoid frequency-encoding-related artifacts, fully phase-encoded methods have been proposed (11–13). One method, known as spectrally resolved fully phase-encoded three-dimensional (3D) fast spin-echo (SR-FPE), uses a CPMG spin-echo sequence with phase encoding in all three dimensions and temporal sampling across the spin echo. The primary barrier to the clinical implementation of such methods is prohibitively long acquisition times (on the order of hours for a fully sampled acquisition). Although self-calibrated 3D parallel imaging and off-resonance encoding methods have been proposed to accelerate SR-FPE (11,14), clinically acceptable acquisition times (<10 min) are not yet feasible.

Both frequency and fully phase-encoded 3D MSI techniques rely on self-calibrated parallel imaging to reduce acquisition time (15). However, a substantial amount of time is spent acquiring fully sampled calibration regions at each of the radiofrequency (RF) offsets. Fully

phase-encoded 3D MSI techniques rely on sampling schemes that are highly undersampled in all three phase dimensions. As a result, the relative portion of time spent on self-calibration for 3D parallel imaging is substantially greater than for two-dimensional (2D) parallel imaging methods that accelerate conventional frequency-encoded 3D data sets.

The purpose of this work is to develop a strategy for externally calibrated parallel imaging near metallic implants. To enable this, a rapid calibration method using a broadband RF excitation, ultrashort echo time (UTE), and fully phased-encoded imaging is proposed. Externally calibrated PMRI near metallic implants is demonstrated in phantoms and in vivo using both frequency-encoded and fully phase-encoded methods.

THEORY

Externally Calibrated Versus Self-Calibrated Sampling Strategies for 3D-MSI

In 3D-MSI techniques, the extreme range of off-resonance induced by a metallic implant can be split into more manageable segments, each spanning a smaller frequency bandwidth (Fig. 1a). With 3D-MSI, separate frequency-encoded or fully phase-encoded 3D-FSE acquisitions are performed for each RF offset. These segments are combined to form a composite image spanning the entire range of frequencies.

Self-calibrated parallel imaging can be used to accelerate 3D-MSI acquisitions (15). In frequency-encoded methods, 2D parallel imaging acceleration can be performed in the k_y and k_z dimensions (Fig. 1b). With 3D phase-encoded methods, parallel imaging can be performed in all three phase-encoding directions. In either case, fully sampled calibration data are acquired for each RF offset.

The acquisition of calibration regions for all of the RF frequency offsets of a 3D-MSI acquisition is time-consuming. The problem exacerbated when moving from frequency-encoded methods to less efficient fully phase-encoded methods in which calibration data are acquired point-wise for each RF frequency offset. Consider the case of a modest 18 × 18 × 18 calibration and 24 RF offsets. Acquisition of these calibration data require 139968 samples, and would take approximately 15 min using SR-FPE with an echo spacing of 6.5 ms. Multiband excitations can reduce the number of RF offsets required for a given spectral coverage by simultaneously exciting the signal from multiple RF offsets (16). Assuming that a triband excitation was used, calibration would take approximately 5 min. Similarly, the default calibration region (elliptical 32 × 16, 24 RF offsets) of the product MAVRIC sequence (frequency-encoded 3D-MSI method) would require approximately 1 min.

For these reasons, the use of a single external calibration for all RF offsets used in MSI methods would be a far more efficient strategy, particularly for fully phase-encoded methods. The use of a single external calibration requires that calibration data be acquired rapidly with minimal artifact. With this approach (Fig. 1c), the entire 3D-MSI acquisition, including the central region of k-space, can be heavily undersampled for each RF offset, offering substantial reductions in acquisition times. To achieve this goal, we developed an external-calibration technique using a fully phase-encoded UTE acquisition.

Requirements of External Calibration

Metallic implants with a high magnetic susceptibility (eg, stainless steel and cobalt-chromium-molybdenum) induce off-resonance signal exceeding ± 10 kHz at 1.5 Tesla (T) with even more severe off-resonance at 3T (6,7). Difficulties in exciting the entire off-resonance are substantially greater if the gradients are left on during RF excitation to minimize the TE. In this case, the total off-resonance is the sum of the off-resonance caused by both the system gradients and those induced by the metallic implant. Nonselective RF pulses with low flip angles can be used to excite the entire off-resonance, provided that the bandwidth of the RF pulse is greater than the sum of the off-resonance induced by the gradients and the metallic implant.

Large static gradients in the B_0 field, particularly in regions in close proximity to the metallic implant, lead to increased intravoxel dephasing and rapid T_2^* decay. To excite the signal close to the metallic implant, echo times must be minimized. Fortunately, coil sensitivity images have inherently low spatial resolution, which limits the maximum k-space encoding necessary, allowing for very short echo times.

The combination of frequency encoding and wide bandwidth pulses creates substantial artifact (17). Extreme off-resonance signal induced by the metallic implant and excited by the broadband RF pulse leads to large bulk distortions in the frequency-encoded direction, resulting in the formation of signal loss and signal pileup artifacts.

Broadband Ultrashort Echo Time Fully Phase-Encoded Imaging

To address the aforementioned challenges of imaging near metallic implants (extreme off-resonance, rapid T_2^* decay, and frequency-encoding distortions), a fully phase-encoded calibration acquisition using broadband excitation and ultrashort echo times is introduced. This techniques uses a UTE signal acquisition to capture signal before it has dephased, broadband excitation using low flip angles, and nonselective RF pulses to excite the entire off-resonance spectrum and fully phase-encoded imaging to prevent large in-plane distortions caused by the combination of frequency encoding and broadband excitation. Figure 2 describes the proposed calibration pulse sequence. This acquisition acquires a single point in k-space per pulse repetition time (TR). Each TR has the same echo time, independent of the set of phase-encoding gradients applied for that particular TR. The minimum achievable TE is determined by the resolution of the calibration acquisition and the performance of the system (maximum gradient strength, gradient slew rate). To minimize the echo time, both RF excitation and data acquisition occur while the phase-encoding gradients are on. Unwanted slice selectivity (18) and signal excitation loss near the implant caused by the frequency profile of the RF pulse are limited by restricting the maximum gradient amplitude during RF excitation (“G_{RF}”). Immediately after RF excitation, gradients are ramped.

METHODS

The proposed method was evaluated using phantoms and in vivo experiments. All images were acquired at 3 T (MR 750 GE Healthcare, Waukesha, Wisconsin, USA). In vivo

experiments were performed after obtaining informed consent and approval from the University of Wisconsin Health Sciences Institutional Review Board.

Phantom Experiments

A total hip prosthesis consisting of a Co/Cr/Mo alloy head and titanium stem (Alliance X-Series, Integral Porous Primary Hip System, Biomet Orthopedics, Warsaw, Indiana, USA) was used to construct a total hip replacement phantom.

SR-FPE, MAVRIC, and MAVRIC-SL acquisitions of the total hip replacement phantom were prospectively undersampled using either a self-calibrated sampling Externally Calibrated PMRI Near Metallic Implants 3 pattern (ie, including a fully sampled calibration region at each RF offset, Fig. 1b) or an external-calibration sampling pattern (ie, without a fully sampled calibration region at each RF offset, Fig. 1c) using a 16-channel wrap coil (NeoCoil, Pewaukee, Wisconsin, USA). Furthermore, the central calibration regions of the self-calibrated data sets were retrospectively decimated to generate retrospectively decimated external calibration data sets. SR-FPE acquisitions were acquired using the following parameters: outer acceleration factor = 3 × 2 × 2, autocalibration signal (ACS) = 18 × 18 × 18/0 × 0 × 0 (self-calibrated/external-calibrated), echo train length (ETL) = 24, temporal samples = 34, receiver bandwidth (BW) = ±8.6 kHz, echo spacing = 6.4 ms, 2.3-kHz multiband Gaussian pulses centered at [−4, 0, 4] kHz (16), variable flip angle schedule with max and minimum flip angles of 58° and 10°, 24-kHz spectral coverage, field of view (FOV) = 22.5 × 14.8 × 15.2 cm, matrix = 150 × 100 × 38, TR = 560 ms, TE_{eff} = 47.5 ms, acquisition time- = 46/38 min (self-calibrated/external-calibrated). MAVRIC and MAVRIC-SL acquisitions were acquired with the following parameters: R = 2 × 2, ACS = 32 × 16 elliptical/0 × 0 (self-calibrated/external-calibrated), ETL = 24, BW = ±128 kHz, 2.3-kHz Gaussian pulse, 24-kHz spectral coverage, matrix = 256 × 168 × 38, phantom acquisition time = 7 min 48 s/6 min 25 s (self-calibrated/external-calibrated).

Retrospective In vivo Experiments

Self-calibrated SR-FPE and MAVRIC acquisitions were acquired in a volunteer with a total knee replacement. The calibration region of self-calibrated SR-FPE and MAVRIC acquisitions were retrospectively undersampled to demonstrate the in vivo feasibility.

SR-FPE acquisitions were acquired using the following parameters: outer acceleration factor = 3 × 2 × 2, ACS = 18 × 18 × 18, ETL = 24, temporal samples = 42, receiver BW = ±10.4 kHz, 2.3-kHz multiband Gaussian pulses centered at [−4, 0, 4] kHz, variable flip angle schedule with max and minimum flip angles of 56° and 10°, 18-kHz spectral coverage, matrix = 150 × 100 × 38, FOV = 22.5 × 14.8 × 15.2 cm, TR = 545 ms, TE_{eff} = 47 ms, acquisition time = 28 min. The fully sampled region of this self-calibrated acquisition was retrospectively subsampled to create an externally calibrated sampling pattern that could have been acquired with an acquisition time of 22 min.

MAVRIC acquisitions were acquired with the following parameters: R = 2 × 2, ACS = 32 × 16 elliptical, ETL = 20, TR = 2891 ms, 2.3-kHz Gaussian pulse, 24-kHz spectral coverage, matrix = 160 × 106 × 38, acquisition time = 5 min 10 s. The fully sampled region of this

self-calibrated acquisition was retrospectively subsampled to create an externally calibrated sampling pattern that could have been acquired with an acquisition time of 3 min 11 s.

Prospective In vivo Experiments

Prospectively undersampled self-calibrated SR-FPE, MAVRIC, and 2D-FSE acquisitions were acquired on a volunteer with a total knee replacement. SR-FPE acquisitions were acquired using the following parameters: outer acceleration factor = 3 × 2 × 2, ACS = 18 × 18 × 18, ETL = 24, temporal samples = 42, receiver BW = ±10.4 kHz, 2.3-kHz multiband Gaussian pulses centered at [−4, 0, 4] kHz, variable flip angle schedule with max and minimum flip angles of 56° and 10°, 18-kHz spectral coverage, matrix = 140 × 106 × 30, FOV = 22.5 × 17.1 × 18.0 cm, TR = 545 ms, TE_{eff} = 47 ms, acquisition time = 22 min.

MAVRIC acquisitions were acquired with the following parameters: R = 2 × 2, ACS = 32 × 16 elliptical, ETL = 24, 2.3-kHz Gaussian pulse, 24-kHz spectral coverage, matrix = 160 × 122 × 30, FOV = 22.5 × 17.1 × 18.0 cm, ETL = 24, TR = 4892 ms, acquisition time = 4 min 34 s.

For comparison, a multislice 2D-FSE acquisition was also acquired with the following parameters: FOV = 22.5 × 22.5 cm, matrix size = 256 × 256, slices = 30, slice thickness = 4 mm, TR = 4000 ms, ETL = 24, BW = ±143 kHz, TE_{eff} = 8.8 ms, NEX = 2, scan time = 3 min 28 s.

Calibration Acquisition

For all externally calibrated acquisitions (phantom and in vivo SR-FPE, MAVRIC, and MAVRIC-SL acquisitions), an additional parallel imaging calibration acquisition was performed using the proposed broadband fully phase encoded UTE sequence. The following acquisition parameters were used: 8-μs hard pulse (150-kHz excitation bandwidth), G_{RF} = 9 mT/m, TE = 80 μs, TR = 1.1 ms, matrix size = 31 × 31 × 31 with elliptical k-space sampling, flip angle = 2°, acquisition time = 23 s.

Image Reconstruction

All image reconstructions were performed using MATLAB (v2014, The MathWorks, Natick, Massachusetts, USA) on iMac workstations (Apple Computer, Cupertino, California, USA). For both externally calibrated and self-calibrated MAVRIC acquisitions, autocalibrated reconstruction of Cartesian data (ARC) reconstruction (19) was performed using a 3 × 7 × 7 kernel. For both externally calibrated and self-calibrated SR-FPE, source images of each temporal SR-FPE data set were reconstructed using a 3D undersampled GRAPPA (20) reconstruction and a kernel size of 7 × 5 × 5. Complex fitting of the temporal SR-FPE data were performed pixel-wise using a nonlinear gradient-based least squares algorithm (lsqnonlin, MATLAB, The MathWorks, Natick, Massachusetts, USA) to generate a signal image, B_0 field map, and R_2^* decay map (11).

RESULTS

SR-FPE, MAVRIC, and MAVRIC-SL acquisitions using self-calibrated, retrospectively decimated externally calibrated, and prospectively acquired externally calibrated parallel imaging of a total hip replacement phantom are shown in Figure 3. Externally calibrated SR-FPE, MAVRIC, and MAVRIC-SL acquisitions offer similar image quality when compared with the reference standard of self-calibrated parallel imaging. Difference maps between externally calibrated and self-calibrated images show the minimum effect of additional subsampling and external calibration. Larger differences are seen between prospectively acquired, externally calibrated images and self-calibrated images. These differences are caused by differences in sampling patterns, view ordering schemes, and the resulting differences in the evolution of the magnetization. Significant reductions in acquisition times were seen when moving from self-calibrated to externally calibrated acquisitions, 8-min reduction for SR-FPE, and a 83-s reduction for MAVRIC and MAVRIC-SL. Furthermore, the feasibility of externally calibrated parallel imaging in the absence (MAVRIC) or presence (MAVRIC-SL) of a slice-selective gradient was also demonstrated in this example.

Figure 4 compared the self-calibrated and retrospectively undersampled, externally calibrated parallel imaging for a volunteer with a total knee replacement. SR-FPE and MAVRIC acquisitions acquired with self-calibrated parallel imaging sampling patterns were retrospectively decimated to simulate the externally calibrated acquisitions. When compared with the self-calibrated parallel imaging, externally-calibrated SR-FPE and MAVRIC acquisitions both offered similar image quality with reduced acquisition times. Externally calibrated SR-FPE resulted in a 6-min reduction in acquisition time, whereas externally calibrated MAVRIC offered a 2-min reduction.

Figure 5 shows an example of a prospectively undersampled example of externally calibrated SR-FPE and MAVRIC acquired in a volunteer with a total knee replacement. Prospectively undersampled, externally calibrated SR-FPE and MAVRIC acquisitions are shown and compared with traditional 2D-FSE. Both SR-FPE and MAVRIC show substantial improvements in imaging the tissue directly adjacent to the knee prosthesis, with minimal distortion and less signal dropout.

DISCUSSION

In this work, we developed a new strategy for externally calibrated parallel imaging near metallic implants. By using a fully phase-encoded calibration acquisition with broadband RF excitation and ultrashort echo times, parallel imaging calibration data for all RF offsets of a 3D-MSI acquisition were acquired within a single acquisition. Removing the requirement to acquire calibration data at every RF offset enables substantial time-savings, particularly for fully phase-encoded methods such as SR-FPE. Our external-calibration approach was validated through comparisons with self-calibrated parallel imaging in a retrospectively decimated and prospectively undersampled phantom study and a retrospectively undersampled in vivo study in a volunteer with a total knee replacement. Furthermore, this approach was demonstrated through a prospectively undersampled in vivo study of a volunteer with a total knee replacement.

The proposed calibration technique was insensitive to the presence or absence of a slab-selective gradient in a 3D-MSI acquisition (ie, MAVRIC-SL and MAVRIC, respectively). Using slab selection for each RF offset in 3D-MSI excites spins at locations where the sum of off-resonance from both the slice-selective gradient and the metallic implant falls within the excitation bandwidth. Sveinsson et al (21) recently proposed an approach to further accelerate 3D-MSI techniques that use a slice-selective gradient (SEMAC or MAVRIC-SL) by reconstructing hexagonally undersampled k-space patterns rather than fully sampled k-space patterns. Provided that the FOV is larger than the extent of the implant distortions, the aliasing artifact will not interfere with intended image and can easily be removed using a post-processing masking step. Our proposed technique should be compatible with the hexagonal sampling approach, as reconstructing aliased images will allow higher acceleration factors regardless of whether self or external-calibration is used. However, the acquisition-time improvements for externally calibrated hexagonal sampling patterns would be smaller, because the calibration region is already undersampled.

Motion between calibration and imaging acquisitions will cause artifacts in externally calibrated parallel imaging techniques (22). Artifacts resulting from motion between calibration and imaging acquisitions were not apparent in the knee examples shown. However, this technique might cause artifacts in anatomic locations that are more prone to motion.

Despite substantial reductions in acquisition times through the use of externally calibrated parallel imaging, further acceleration is still required to translate fully phase-encoded methods like SR-FPE into the clinical setting. Optimization of pulse-sequence design, such as strategies to reduce the FOV (8,23) and optimization of multiband excitations (16), are complementary methods that could be used to further accelerate acquisitions. Furthermore, improvements in reconstruction techniques through the use of compressed sensing (12,24), hexagonal undersampling (21), and/or off-resonance encoding (14) could also accelerate acquisitions.

Acquisition of a single high-resolution fully phase-encoded UTE acquisition rather than a low-resolution calibration and a 3D-MSI acquisition may also be a viable option for in vivo imaging near metal (25). The fully phase-encoded UTE sequence is substantially faster than fully phase-encoded spin-echo based sequences like SRFPE. Furthermore, wide bandwidth pulses would improve the spectral coverage, allowing imaging of tissue closer to the metallic implant, provided that the T_2^* decay is not too rapid. However, peak B_1 constraints limit the maximum attainable flip angles of broadband RF pulses, and as a result, limits the amount of T_1 weighting that can be achieved.

CONCLUSIONS

In conclusion, a fully phase-encoded acquisition with broadband excitation and UTE is a viable approach for externally calibrated parallel imaging for 3D-MSI, eliminating the need for independent calibration regions for each RF offset. Significant reductions in acquisition time can be achieved, particularly for fully phase-encoded methods like SR-FPE.

Acknowledgments

The authors thank Dr. Kevin Koch for valuable discussions and GE Healthcare for research support. We also wish to thank the NIH (UL1TR000427) for its support of a pilot grant administered by the University of Wisconsin Institute for Clinical and Translational Research (ICTR), and the support of the Natural Sciences and Engineering Research Council of Canada (NSERC) Postdoctoral Fellowship Program.

References

1. Kurtz S, Mowat F, Ong K, Chan N, Lau E, Halpern M. Prevalence of primary and revision total hip and knee arthroplasty in the United States from 1990 through 2002. J Bone Joint Surg Am. 2005; 87(z):1487–1497. [PubMed: 15995115]
2. White LM, Kim JK, Mehta M, Merchant N, Schweitzer ME, Morrison WB, Hutchison CR, Gross AE. Complications of total hip arthroplasty: MR imaging-initial experience. Radiology. 2000; 215(1):254–262. [PubMed: 10751496]
3. Hayter CL, Koff MF, Potter HG. Magnetic resonance imaging of the postoperative hip. J Magn Reson Imaging. 2012; 35(5):1013–1025. [PubMed: 22499278]
4. Toms AP, Marshall TJ, Cahir J, Darrah C, Nolan J, Donell ST, Barker T, Tucker JK. MRI of early symptomatic metal-on-metal total hip arthroplasty: a retrospective review of radiological findings in 20 hips. Clin Radiol. 2008; 63(1):49–58. [PubMed: 18068790]
5. Schenck JF. The role of magnetic susceptibility in magnetic resonance imaging: MRI magnetic compatibility of the first and second kinds. Med Phys. 1996; 23(6):815–850. [PubMed: 8798169]
6. Smith MR, Artz NS, Wiens C, Hernando D, Reeder SB. Characterizing the limits of MRI near metallic prostheses. Magn Reson Med. 2015; 74:1564–1573. [PubMed: 25483410]
7. Koch KM, King KF, Carl M, Hargreaves BA. Imaging near metal: the impact of extreme static local field gradients on frequency encoding processes. Magn Reson Med. 2014; 71(6):2024–2034. [PubMed: 23843341]
8. Koch KM, Lorbiecki JE, Hinks RS, King KF. A multispectral three-dimensional acquisition technique for imaging near metal implants. Magn Reson Med. 2009; 61(2):381–390. [PubMed: 19165901]
9. Lu W, Pauly KB, Gold GE, Pauly JM, Hargreaves BA. SEMAC: slice encoding for metal artifact correction in MRI. Magn Reson Med. 2009; 62(1):66–76. [PubMed: 19267347]
10. Koch KM, Brau AC, Chen W, Gold GE, Hargreaves BA, Koff M, McKinnon GC, Potter HG, King KF. Imaging near metal with a MAVRIC-SEMAC hybrid. Magn Reson Med. 2011; 65(1):71–82. [PubMed: 20981709]
11. Artz NS, Hernando D, Taviani V, Samsonov A, Brittain JH, Reeder SB. Spectrally resolved fully phase-encoded three-dimensional fast spin-echo imaging. Magn Reson Med. 2014; 71(2):681–690. [PubMed: 23483631]
12. van Gorp JS, Bakker CJ, Bouwman JG, Smink J, Zijlstra F, Seevinck PR. Geometrically undistorted MRI in the presence of field inhomogeneities using compressed sensing accelerated broadband 3D phase encoded turbo spin-echo imaging. Phys Med Biol. 2015; 60(2):615–631. [PubMed: 25548990]
13. Ramos-Cabrer P, van Duynhoven JP, Van der Toorn A, Nicolay K. MRI of hip prostheses using single-point methods: in vitro studies towards the artifact-free imaging of individuals with metal implants. Magn Reson Imaging. 2004; 22(8):1097–1103. [PubMed: 15527996]
14. Smith MR, Artz NS, Koch KM, Samsonov A, Reeder SB. Accelerating sequences in the presence of metal by exploiting the spatial distribution of off-resonance. Magn Reson Med. 2014; 72(6): 1658–1667. [PubMed: 24431210]
15. Hargreaves BA, Chen W, Lu W, Alley MT, Gold GE, Brau AC, Pauly JM, Pauly KB. Accelerated slice encoding for metal artifact correction. J Magn Reson Imaging. 2010; 31(4):987–996. [PubMed: 20373445]
16. Artz NS, Wiens CN, Smith MR, Hernando D, Samsonov A, Reeder SB. Accelerating fully phase-encoded MRI near metal using multiband radiofrequency excitation. Magn Reson Med. 2016; doi: 10.1002/mrm.26209

17. Koch, KM., King, KF., Carl, M., McKinnon, GC. Comparison of 2D spin-echo, spin-echo multi-spectral imaging, and ultra-wide bandwidth 3D radial techniques for imaging near metal. Proceedings of the 20th Annual Meeting of ISMRM; Melbourne, Australia. 2012. p. 2433
18. Jang H, Wiens CN, McMillan AB. Ramped hybrid encoding for improved ultrashort echo time imaging. Magn Reson Med. 2015; doi: 10.1002/mrm.25977
19. Beatty, P., Brau, A., Chang, S., Joshi, S., Michelich, C., Bayram, E., Nelson, T., Herfkins, R., Brittain, J. A method for autocalibrating 2D-accelerated volumetric parallel imaging with clinically practical reconstruction times. Proceedings of the 15th Annual Meeting of ISMRM; Berlin, Germany. 2007. p. 1749
20. Griswold MA, Jakob PM, Heidemann RM, Nittka M, Jellus V, Wang J, Kiefer B, Haase A. Generalized autocalibrating partially parallel acquisitions (GRAPPA). Magn Reson Med. 2002; 47(6):1202–1210. [PubMed: 12111967]
21. Sveinsson B, Worters PW, Gold GE, Hargreaves BA. Hexagonal undersampling for faster MRI near metallic implants. Magn Reson Med. 2015; 73(2):662–668. [PubMed: 24549782]
22. McKenzie CA, Yeh EN, Ohliger MA, Price MD, Sodickson DK. Self-calibrating parallel imaging with automatic coil sensitivity extraction. Magn Reson Med. 2002; 47(3):529–538. [PubMed: 11870840]
23. den Harder JC, van Yperen GH, Blume UA, Bos C. Off-resonance suppression for multispectral MR imaging near metallic implants. Magn Reson Med. 2015; 73(1):233–243. [PubMed: 24488684]
24. Worters PW, Sung K, Stevens KJ, Koch KM, Hargreaves BA. Compressed- sensing multispectral imaging of the postoperative spine. J Magn Reson Imaging. 2013; 37(1):243–248. [PubMed: 22791572]
25. Koch, KM., McKinnon, G. On the feasibility of overcoming frequency encoding limitations near metal implants with broadband single-point imaging on clinical MR systems. Proceedings of the 22nd Annual Meeting of ISMRM; Milan, Italy. 2014. p. 1679

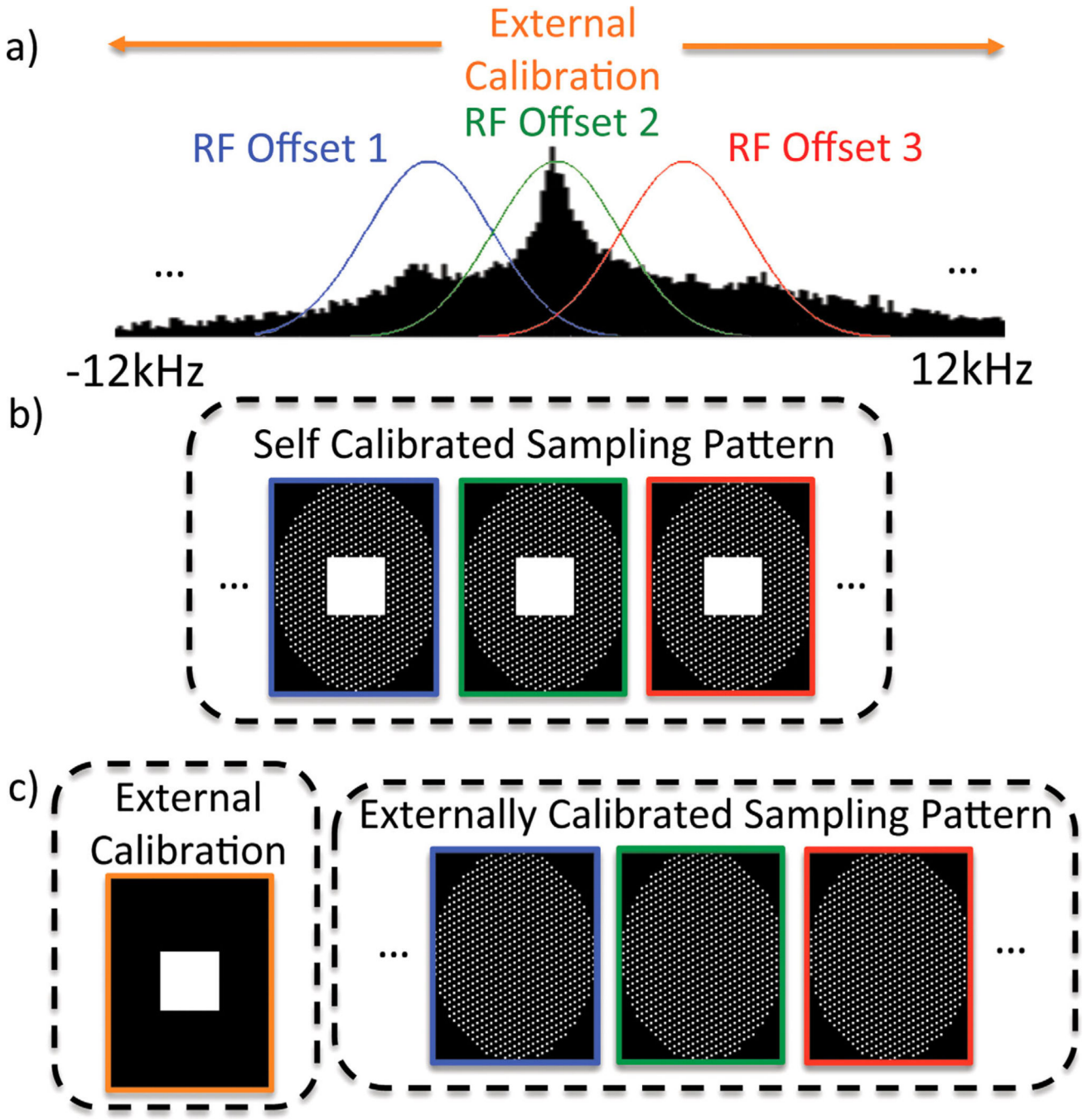

FIG. 1.

(a) External calibration using a fully phase-encoded UTE acquisition with broadband excitations spanning the extremely large off-resonance signal induced by metallic implants, which can be used for parallel imaging calibration across all RF offsets (colored Gaussians) of a 3D-MSI acquisition. (b) Self-calibration requires fully sampled calibration regions at each RF offset. (c) External-calibration acquires the fully sampled calibration region only once, allowing for a reduction in data sampling for all RF offsets and shorter scan times.

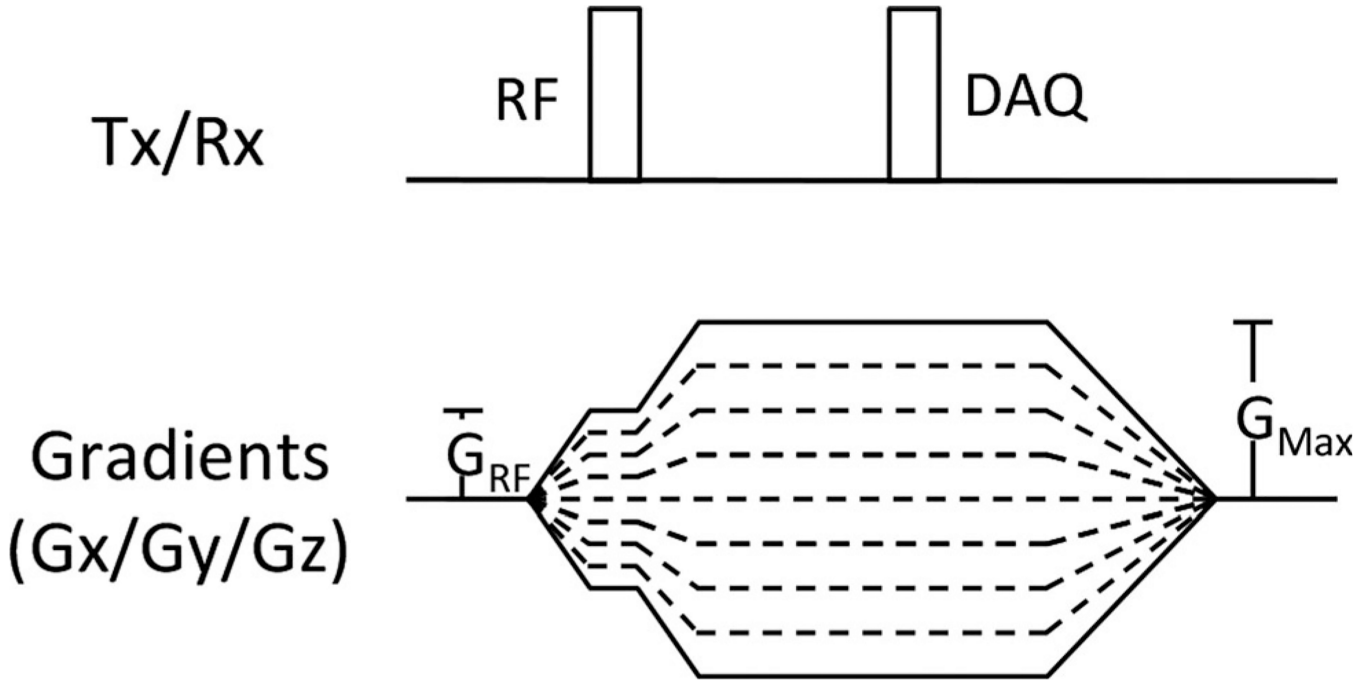

FIG. 2.

Pulse sequence diagram of the proposed external calibration acquisition. The maximum gradient amplitude during RF excitation is limited to a maximum value of G_{RF} to prevent slice-selectivity artifacts and signal excitation loss near metallic implants. Immediately after excitation, gradients are ramped, allowing calibration acquisitions with ultrashort echo times.

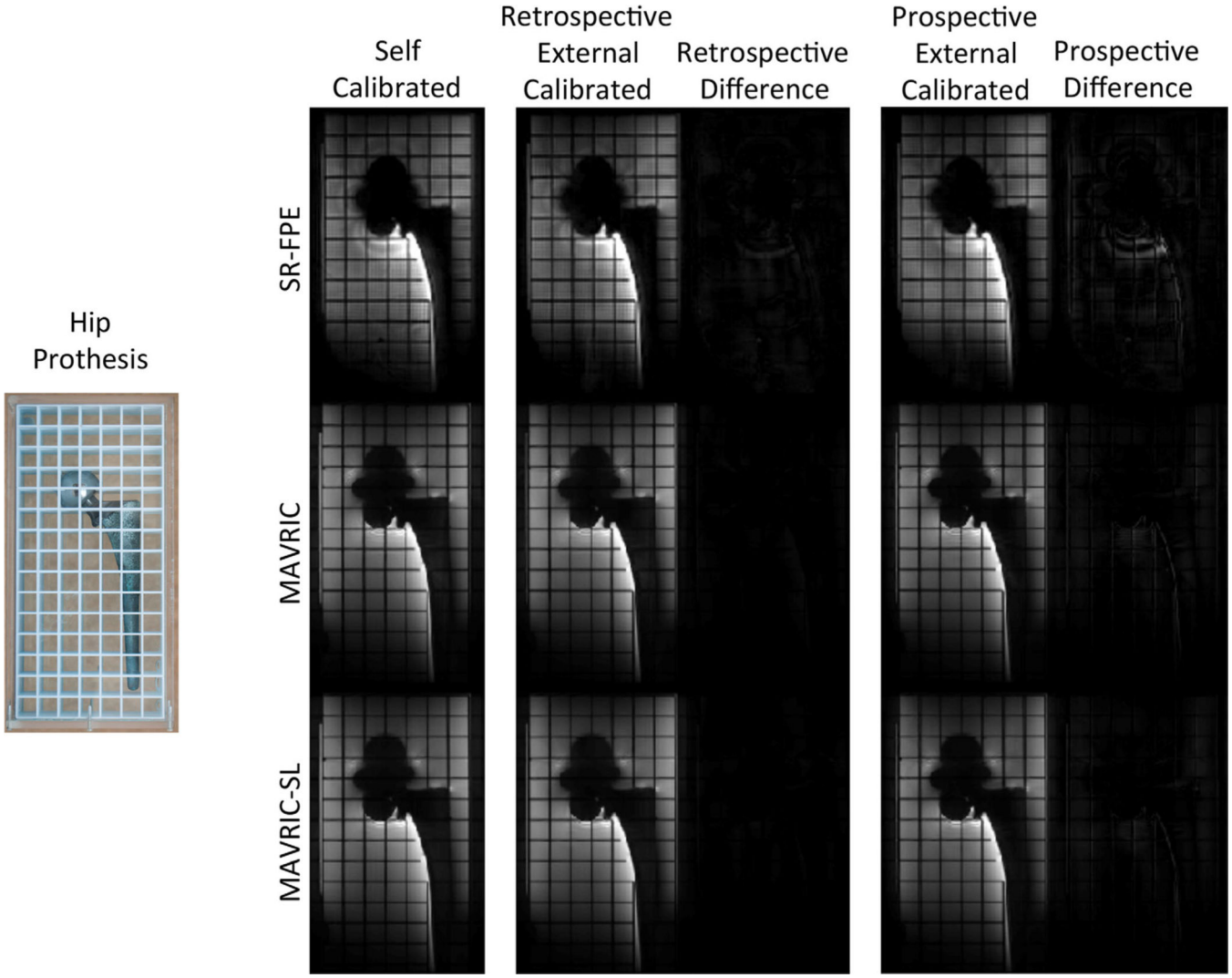

FIG. 3.

SR-FPE, MAVRIC, and MAVRIC-SL acquisitions using both self and externally calibrated parallel imaging (both retrospectively decimated self-acquired and prospectively acquired) are shown on a total hip replacement phantom, demonstrating reductions in acquisition time of approximately 25% (8 min for SR-FPE and 83 s for MAVRIC and MAVRIC-SL). The higher net acceleration factor and the external calibration process caused relatively small differences between self-calibrated and retrospectively decimated externally-calibrated acquisitions. Different sampling patterns, view-ordering schemes, and the resulting differences in the evolution of the magnetization in the echo train caused larger differences in self-calibrated and prospectively acquired, externally calibrated acquisitions.

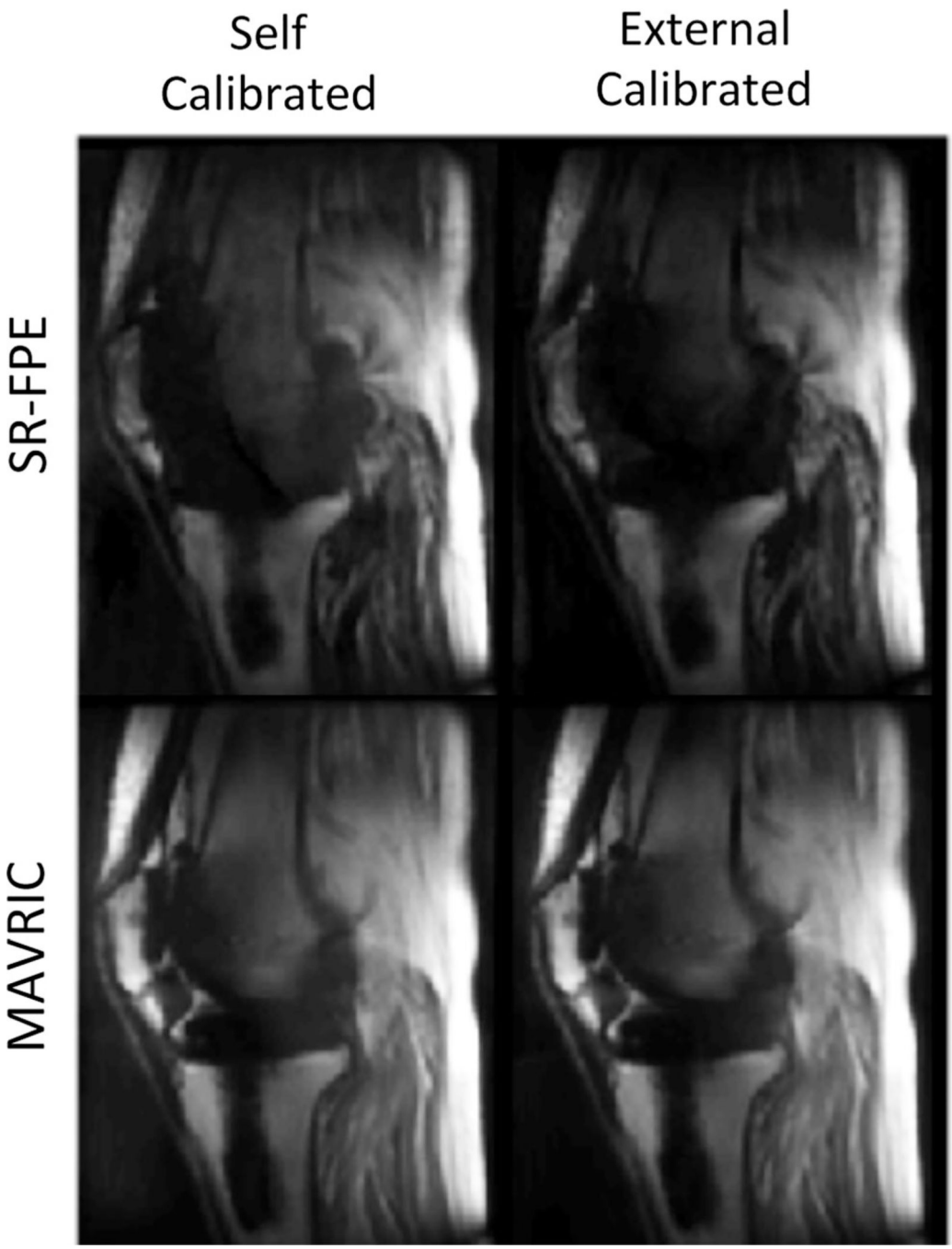

FIG. 4.

In vivo knee acquisitions show externally calibrated SR-FPE and MAVRIC acquisitions with equivalent image quality as self-calibrated but with substantial time savings. The calibration region of self-calibrated SR-FPE and MAVRIC acquisitions were retrospectively undersampled to demonstrate in vivo feasibility of externally calibrated parallel imaging in a volunteer with a total knee replacement. Reductions in acquisition time were 6 min for SR-FPE and 2 min for MAVRIC.

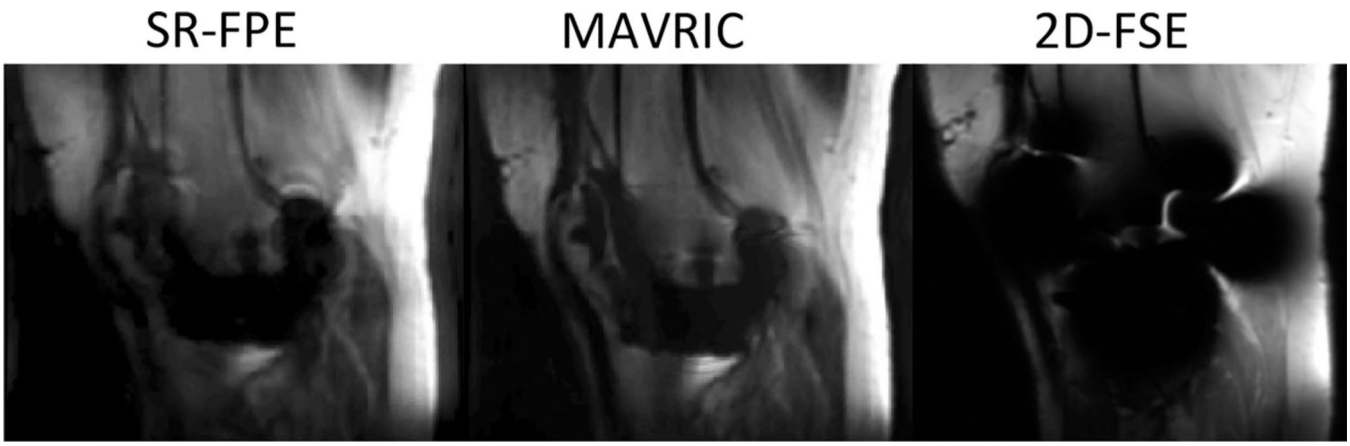

FIG. 5.

Prospectively undersampled, externally calibrated SR-FPE and MAVRIC acquisitions of a volunteer with a total knee replacement. Both MAVRIC and SR-FPE improved visualization of tissue near the implant compared with a traditional 2D-FSE acquisition.